

Research Space

Journal article

Ammonia and temperature sensing applications using fluorometric and colorimetric microparticles and polymeric films doped with BODIPY-emitters

Bertolo, E., Beatriz S. Cugnasca, Frederico Duarte, Hugo M. Santos, José Luis Capelo-Martínez, Alcindo A. Dos Santos and Carlos Lodeiro

This is the author's accepted version of the article published as: Cugnasca, B.S., Duarte, F., Santos, H.M. *et al.* Ammonia and temperature sensing applications using fluorometric and colorimetric microparticles and polymeric films doped with BODIPY-emitters. *Microchim Acta* **191**, 746 (2024). <https://doi.org/10.1007/s00604-024-06814-2>

Ammonia and Temperature Sensing applications using Fluorometric and Colorimetric microparticles and polymeric films doped with BODIPY-emitters

Beatriz S. Cugnasca^{a,b}, Frederico Duarte^b, Hugo M. Santos^b, José Luis Capelo-Martínez^{b,c}, Emilia Bertolo^d, Alcindo A. Dos Santos^{a*} and Carlos Lodeiro^{b,c,d,**}

^a*Institute of Chemistry, Department of Fundamental Chemistry, University of São Paulo, 05508-000 São Paulo, SP, Brazil*

^b*BIOSCOPE Research Group, LAQV-REQUIMTE, Department of Chemistry, NOVA School of Science and Technology, FCT NOVA, NOVA University Lisbon, 2829-516 Caparica, Portugal*

^c*PROTEOMASS Scientific Society, 2825-466 Costa da Caparica, Portugal*

^d*Section of Natural and Applied Sciences, School of Psychology and Life Sciences, Canterbury Christ Church University, CT1 1QU Canterbury, United Kingdom.*

Corresponding authors: *alcindo@iq.usp.br and **cle@fct.unl.pt

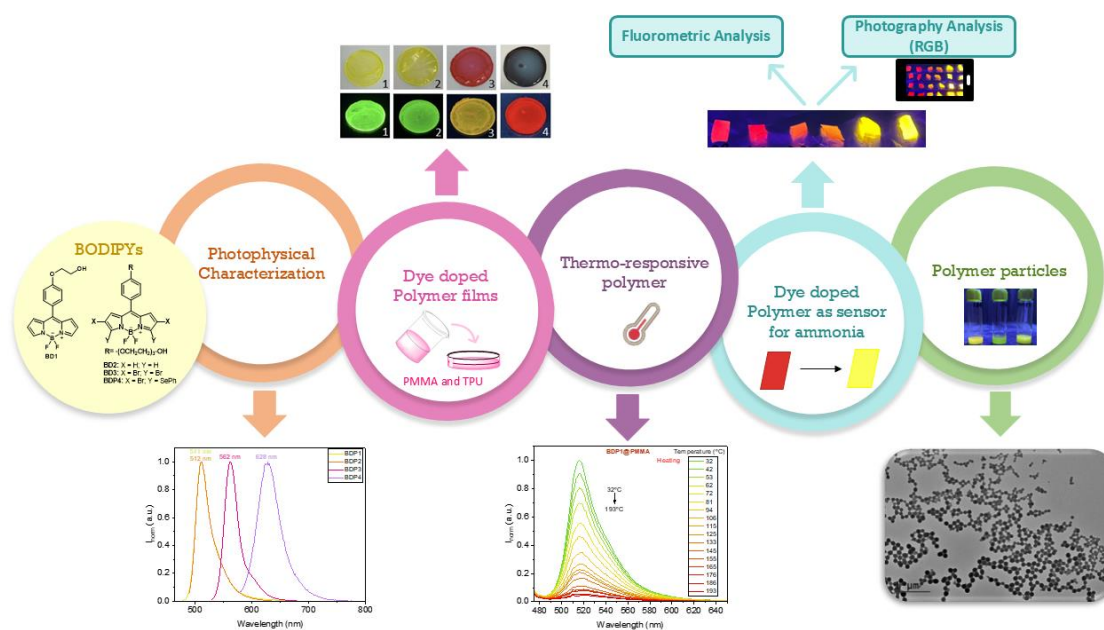
Abstract

In this study we synthesized four functionalized BODIPY derivatives (**BDP1** to **4**) and investigated their optical properties both in solution and when incorporated into a solid matrix. Recognizing the versatility of BODIPY derivatives and the increasing interest in developing new luminescent organic dyes embedded in polymers, the BODIPY derivatives were dispersed into two types of polymeric matrices: Poly(methyl methacrylate) (PMMA) and Thermoplastic Polyurethane (TPU), both as films and microparticles. This resulted in eight new BODIPY-doped polymer films, and eight types of BODIPY-doped polymeric microparticles for use in aqueous solutions. The integration of the BODIPY dyes into the polymeric matrices combines the unique properties of the polymer films, such as porosity, flexibility, and elasticity, with the excellent photophysical characteristics of the BODIPYs. Importantly, the dispersion minimized issues such as aggregation-caused quenching (ACQ) commonly observed in solid-state luminescent materials. The thermometric responses of all polymer films were evaluated by studying their solid-state emission spectra in the 25-200 °C temperature range. The reversibility of these temperature-induced changes was also assessed, revealing excellent recovery of luminescence. These promising results suggest these materials could have applications as fluorescent thermometric sensors.

Furthermore, we explored the potential of the brominated (**BDP3**) and chalcogenated (**BDP4**) BODIPY derivatives as ammonia sensors. The two derivatives produced yellow fluorescent products upon interaction with the analyte. Kinetic studies using solid-state emission spectra of **BDP4@TPU** and **BDP4@PMMA** showed significant differences in reaction rates (minutes for **BDP4@TPU** and hours in the case of **BDP4@PMMA**) attributable to the higher permeability of TPU when compared with PMMA. Detection and quantification of ammonia concentration was conducted by means of a simple photographic analysis, measuring the "R" (red) and "G" (green) components of RGB color parameters; the results from the photographic method correlated well with the results from fluorimetric spectroscopy studies. The photographic analysis is

straightforward, portable, and does not require expensive equipment. Finally, we successfully applied polymeric microparticles doped with BODIPYs to detect ammonia in water, demonstrating their effectiveness without the need for organic solvents. This highlights their potential for environmental monitoring and other applications requiring sensitive and selective detection methods.

Graphical abstract



Keywords

BODIPY, fluorescence probe, polymer films, polymers, PMMA, TPU, sensors, ammonia.

1. Introduction

Interest in the development of new luminescent organic dye-doped polymers has been growing in recent years due to the wide versatility of applications in industries, medicine and analytical process, and is the target of investigation by many researchers.[1] Research has been conducted in their use in organic light-emitting diodes (OLED), inkjet printing, sensors, cellular bioimaging, optical fiber, nanocarriers and in drug delivery, thermometric applications, and contrast agents in medicine, among other applications.[2],[3],[4],[5],[6] The vast majority of π -conjugated chromophores exhibit a high fluorescence emission in dilute solutions. However, when in the solid state, a partial or total quenching of fluorescence is usually observed.[7] This phenomenon can be

attributed to the aggregation-caused quenching (ACQ), also known as the concentration quenching effect, caused by the intense intermolecular interaction $\pi\cdots\pi$ stacking in aromatic systems, which favors decay via non-radiative pathways. Factors such as packing and distance between molecules must be considered to study this phenomenon.[7],[8],[9] In this way, ACQ is often considered a limiting factor for various luminescent applications of solid-state organic dyes. One strategy to overcome this limitation is through the incorporation of dispersed dyes in polymeric films, which allows improvements in some properties of the chromophore in addition to ensuring its solid-state fluorescence and reduces non-emissive aggregates.[8] A crucial point to be considered is dispersion of the dye in the polymeric matrix to prevent aggregation.[10] A second strategy is to synthesize compounds containing bulky groups or insert highly twisted structures[11] that favor the formation of specific emissive aggregates, minimizing the intramolecular rotation and, consequently, the non-radiative relaxation channel, leading to the fluorescence of the compound in a process known as Aggregation-Induced Emission (AIE). [7],[10],[6],[12],[9] However, this second strategy depends on the reactivity of the compounds for structure modifications and it may be more difficult to predict the π -stacking modes only by analyzing the structure, and intermolecular interaction for more complex molecules, being necessary a more detailed investigation.[13],[7]

Currently, temperature-responsive polymers are very important for biological and biomedical applications, such as temperature sensors, bio-separation, drug transport, and food packaging.[14],[15] In this context, nanothermometers have been explored in solution, in solid state and supported in polymeric matrices.[14],[16] In general, the detection and quantification of temperature variations are detected through the variation in fluorescence intensity[15]. Several polymeric matrices have been studied, including poly(*N*-isopropylacrylamide) (PNIPAAm), poly(*N,N*-diethylacrylamide) (PDEAAm), poly(*N*-vinylcaprolactam) (PVCL), and PMMA.[2],[17],[18],[19].

In addition to being soft and flexible, typical characteristics of polymeric particles include porosity, biodegradability, the ability to swell, soft interface and interior, and easy adjustment of shape and size.[20] All these properties make polymeric particles promising tools in biomedical applications, eg. to be used as carriers for drug/dye delivery.[6] Organic dyes can be incorporated into these particles through different methods, either inside or onto the surface; these dye-doped polymer particles can be used

in biological and medical applications such as cellular bioimaging and theranostics.[6] Biocompatible and biodegradable matrices can be used in the construction of polymeric devices[21] and thus can be used as nanocarriers, with the advantage of being eliminated from the organism after the drug is released. The vast majority of organic dyes have low solubility in aqueous systems, which often limits their applications in biological systems. Thus, the combination of the luminescent properties of the fluorophores and the biocompatibility brought in by the polymeric particles, in addition to ensuring water solubility, allows their use in aqueous medium, with less probability of degradation in the cellular medium compared to the use of free dye. Limitations such as lack of resistance to acid, base, and enzyme attack can be controlled by choosing the appropriate polymeric matrix, in addition to allowing biocompatibility, and maintaining the properties of the fluorophore.[20]

Ammonia (NH₃) is a gas widely used in industry to produce nitrogen-containing compounds. It is estimated that the annual production of ammonia is 176 million tonnes, most of which is obtained through the Haber Bosch process.[22] Ammonia is a colorless irritating gas with a pungent odor, highly soluble in water.[23] When inhaled, it can lead to nasal, eye and respiratory tract irritation, leading to pulmonary dysfunction. Concentrations between 2500 and 4500 ppm can lead to death in 30 minutes; concentrations above 5000 ppm can be rapidly fatal after a few minutes and lead to rapid respiratory arrest.[24] Ammonia is also produced through natural sources, as part of the nitrogen cycle, through processes of organic matter decomposition. It is used in agricultural, mining processes, in cleaning products, and thus can be very present in people's daily lives and/or their workplace. Thus, it is important to develop effective sensors for ammonia, both in its gaseous form and in solution ($\text{NH}_3 + \text{H}^+ \rightleftharpoons \text{NH}_4^+$).[23]

4,4-difluoro-4-bora-3a,4a-diazas-indacene (BODIPY) is a class of chromophores that exhibit excellent photophysical properties. They are very versatile compounds with easy functionalization of the nucleus, which generally have high coefficients of molar absorptivity, high fluorescence quantum yields, low toxicity, as well as absorption and emission spectra in the visible light region. Due to these characteristics, BODIPYs are promising candidates for biological and biomedical applications.[25] However, despite the high fluorescence quantum yield in diluted solutions, BODIPYs tend to aggregate in the solid state due to the intermolecular π - π stacking, resulting in low Φ_F values in the solid state.[26]

Based on our previous work in organic dye-doped polymers[27],[28],[29] and fluorescent sensors based on BODIPYs[30],[31],[32] and knowing the excellent properties of these chromophores, in this work, four BODIPYs containing different functionalizations (polyethylene glycol (PEG) chain, bromide and selenium groups) (Fig. 1) were dispersed in polymeric films of PMMA or TPU (Irogran[®]), to evaluate their photophysical and thermometric properties. Furthermore, we explored their potential use as solid-state ammonia sensors, for possible industrial applications. Due to the color variations, the parameters “R” (red) and “G” (green) of the RGB coloring pattern were extracted from the obtained images, using software, and linear correlations with the NH₄OH concentration were obtained. Finally, due to the high hydrophobicity of the BODIPY derivatives, the compounds were incorporated into polymeric particles and their properties studied, to explore their ability to detect ammonia in aqueous solution.

2. Experimental section

2.1. Materials

The BODIPY **1**,[30] **2**,[31] **3**,[32] and **4**[32] were synthesized through a procedure described in previous work. Poly(methyl methacrylate, PMMA (MW ~ 350,000, T_g 105°C), ammonium hydroxide (NH₄OH), hydrochloric acid, tetrahydrofuran anhydrous ≥ 99.9% and chloroform anhydrous ≥ 99.9% were purchased from Sigma-Aldrich. IROGRAN[®] A 92 P 4637: Polyether-based Thermoplastic Polyurethane Irogran[®] (TPU) was offered by Huntsman (Germany). The perfluoroalkoxy (PFA) supports (5 cm diameter) used in the preparation of the polymer films were purchased from Bohlender, GmbH, Germany. Milli-Q ultrapure water was used in the experiments. All chemicals were of analytical grade and used as received, without purification.

The stock solutions of BODIPYs were prepared in THF (ca. 0.5 mmol/L) in a 1 mL volumetric flask. The absorption and emission spectra of BODIPYs solutions were conducted at 298 K. Quartz cuvettes (3 mL) were used in these experiments. Solutions of NH₄OH (5.0, 2.5, 1.0, 0.5 mol/L) were prepared by diluting appropriate amounts of the stock solution in water, using 10 mL volumetric flasks.

2.2. Absorption and emission spectra

Absorption spectra were recorded on a JASCO V-650 spectrophotometer and the fluorescence emission spectra on a HORIBA JOBIN YVON FluoroMax-4 Spectrofluorometer (PROTEOMASS-BIOSCOPE facility). To obtain the luminescence emission spectra of polymer films doped with BODIPYs, fiber-optics were connected to the spectrofluorometer. Temperature-dependent emission studies were conducted using a hot plate containing a thermocouple. To obtain emission spectra at different temperatures, in heating and cooling cycles, the polymer films doped with BODIPYs were placed on the hotplate and, after temperature stabilization, emission spectra using suitable excitation wavelengths were obtained. The emission spectra of polymeric particles and the fluorescence quantum yield of BODIPYs were recorded on a RF-5301PC spectrofluorophotometer Shimadzu (Institute of Chemistry – University of São Paulo), using quartz cuvettes. Absorption spectra of polymeric particles were recorded on a Cary 60 UV-Vis Agilent Technologies spectrophotometer (Institute of Chemistry – University of São Paulo).

2.3. Characterization of polymeric particles

The polymeric particles were characterized by Dynamic Light Scattering (DLS), zeta potential (ζ), absorption and emission spectra, and analysis by Transmission Electron Microscopy (TEM). Zeta potential and particle size distribution results for polymer particles were performed in a Malvern Instruments Zetasizer Nano series (Nano - ZS) (Institute of Chemistry – University of São Paulo), using a scattering angle of 90°, 298 K and disposable cuvettes. For measurement of zeta potential, a dip cell was used. The stock solutions of dye-doped polymeric particles (50 μ L) were diluted in 1 mL of Milli-Q water for measurement.

Transmission electron microscopy (TEM) experiments were conducted in a TEM JEOL Jem 2100 (Analytical Center of IQ-USP). The sample preparation for TEM consisted of a first stage of hydrophilization of the carbon grid (Support Films, Carbon Type-B - C/B, 200 mesh Cu – TED PELLA, INC, Lot #260218, 01811) in a PELCO easiGlow (15 mA for 25 seconds). After this procedure, 4 μ L of the PMMA polymeric particle solution was applied to the surface of the grid, leaving it to rest for 1 minute. Then, the excess was removed with filter paper and the grid was left to air dry, covered with aluminum foil for 24 hours. For TPU particles, a wash step was conducted before

the application of the sample to the grid's surface. This procedure consisted of centrifuging 500 μ L of the aqueous solution containing the particles for 5 min at 7000 rpm (in a mySPIN 12™ Mini centrifuge from Thermo Fisher Scientific). After this period, the supernatant was removed and 500 μ L of Milli-Q water was added to the pellet. The pellet was resuspended using a vortex (Vortex Mixer LGC). The washing step was performed 3 times. At the end, the colloidal suspension obtained was filtered. After this procedure, 4 μ L of the suspension was applied to the surface of the grid, leaving it to rest for 1 minute. Then, the excess was removed with filter paper and the grid was left to air dry, covered with aluminum foil for 24 hours. The particle size was measured with the aid of the "ImageJ" software.

2.4. High-Resolution Mass Spectrometry (HRMS)

High-Resolution Mass Spectrometry analyses were carried out in the Laboratory for Biological Mass Spectrometry–Isabel Moura (PROTEOMASS Scientific Society Facility), using UHR ESI-Qq-TOF IMPACT HD (Bruker-Daltonics, Bremen, Germany). Compounds were dissolved in 50% (v/v) Acetonitrile containing 0.1% (v/v) aqueous formic acid to obtain working solutions ranging from 0.1 to 1 μ g/mL. Mass spectrometry analysis was carried out by the direct infusion of the compound solutions into the ESI source. MS data were acquired in positive polarity over the range of 250 – 2000 m/z. (Capillary voltage: 4500 V, End plate offset: -500 V, Charging voltage: 2000 V, Corona: 0 nA, Nebulizer gas: 0.3 Bar, Dry Heater: 220 °C, Dry gas: 3.5 L/min). Compass IsotopePattern software was used to obtain the compounds' theoretical mass values, and the spectra are available in Support Information.

2.5. Preparation of BODIPYs-doped polymer films

Initially, PMMA (100 mg) was solubilized in 10 mL of CHCl_3 , under mild heating (50 °C) and stirring, for 15 minutes to favor the solubilization of the polymer. Then, 1 mL of BODIPY solution, previously solubilized in chloroform (0.52 mM) was added to the polymeric solution. The final solution obtained was kept under stirring for 5 minutes, ensuring total solubilization of the dye and, subsequently, added to a PFA support (Bohlander, GmbH, Germany). The support containing polymer solution with BODIPY was kept under circular agitation in an orbital shaker (Elmi DOS-20M) (RPM = 40, orbital rotation) for 24 hours, covered with perforated aluminum foil, ensuring uniform evaporation of the solvent.

To prepare TPU films, the polymer (100 mg) was solubilized in 10 mL of THF for 24 hours, under slight agitation, without heating, avoiding the formation of bubbles. Subsequently, 1 mL of BODIPY solution (0.52 mM), previously solubilized in THF, was added to the polymeric solution. After 5 minutes of stirring, the polymeric solution containing BODIPY was added to the PFA support. The support containing polymer solution with BODIPY was kept under circular agitation on an orbital shaker (RPM = 40) for 24 hours, covered with perforated aluminum foil, ensuring uniform evaporation of the solvent. These procedures were carried out for all BODIPYs used in this work.

2.6. Encapsulation of BODIPYs compounds in polymeric particles

Initially, PMMA (25 mg) was solubilized in 2 mL of THF, under heating (50 °C) and stirring for 15 minutes until complete solubilization of the polymer. Subsequently, the polymeric solution was added to BODIPY, resulting in a final solution of 1 mM. The solution was stirred until complete solubilization of the BODIPY (1 minute). After this period, 600 µL of this solution was added quickly and in one step, to a flask containing 2.4 mL of Milli-Q water under stirring, maintaining 20% of THF in water in the final mixture. It was left stirring for 5 minutes and, subsequently, a filtering step was conducted. Finally, the flask was kept at rest and open for 24 hours to ensure evaporation of all THF and the polymeric particles containing BODIPY encapsulated inside were obtained.

To prepare TPU-based particles, first, the polymer (100 mg) was solubilized in 10 mL of THF for 24 hours, under slight agitation, without heating, avoiding the formation of bubbles. Then, the polymeric solution was added to BODIPY, resulting in a final solution of 1 mM. The solution was stirred until the solubilization of the BODIPY was complete. After this period, 600 µL of this solution was added quickly and in one step, to a flask containing 2.4 mL of Milli-Q water under stirring, maintaining 20% of THF in water in the final mixture. It was left stirring for 5 minutes and, subsequently, a filtering step was conducted. Finally, the flask was kept at rest and open for 24 hours to ensure evaporation of all THF and the polymeric particles containing BODIPY encapsulated inside were obtained.

2.7. Fluorescence quantum yield

The fluorescence quantum yields of BODIPYs were obtained in THF through the following Equation 1.

$$\Phi_s = \Phi_r \left(\frac{A_r}{A_s} \right) \left(\frac{E_s}{E_r} \right) \left(\frac{n_s}{n_r} \right)^2 \text{ (Equation 1)}$$

Φ = fluorescence quantum yield; A = the absorbance at excitation wavelength of solution; E = area under the emission curve, η = refractive index of the solvent. “s” e “r” denotes sample and standard, respectively.[33]

2.8. Kinetic studies with NH_4OH

The kinetic studies with NH_4OH were conducted also through photographic images. First, the polymers **BDP4@TPU** and **BDP4@PMMA** were cut into 1cm×1cm squares and dipped into solutions of NH_4OH of different concentrations (0.5 to 5.0 mol/L). Then, after a specific time, readings were taken using a spectrofluorometer. In parallel, images of the polymers were obtained under visible light and under UV light, using an iPhone 14[®] cell phone inside a lighting control box. The images were analyzed using the software GIMP 2.10.24 and the “R” and “G” values from RGB pattern of color were obtained, allowing us to quantify the variation in the color of polymers when in the presence of different concentrations of the analyte after different reaction times. The RGB values obtained were converted into Yxy values using the website “easyRGB” (<https://www.easyrgb.com/en/>) and the CIE chromaticity diagrams were plotted with Spectra Lux Software v.2.0, Ponto Quântico Nanodispositivos / RENAMI, 2003, P.A. Santa-Cruz, F.S. Teles.

3. Results and discussion

In our recent work,[30],[32],[31] we have developed and synthesized four novel BODIPYs derivatives (**BDP1-BDP4**) (Fig. 1). The BODIPYs nuclei **BDP1** and **BDP2** were synthesized through adaptation of procedures described in the literature; **BDP3** was obtained from **BDP2** in a tetrabromination reaction using NBS in dichloromethane. [32] The chalcogenated **BDP4** was synthesized from **BDP3** through a selenylation reaction, using benzoselenol generated in situ from a $NaBH_4 / Ph_2Se_2$ system; this procedure allows the synthesis of BODIPY derivatives containing selenium groups and bromine in the final structure.[32] All compounds were previously characterized by NMR 1H , ^{13}C , (^{77}Se for **BDP4**), HRMS, melting point, presenting high degree of purity for studies in polymeric matrices.[30],[32],[31]

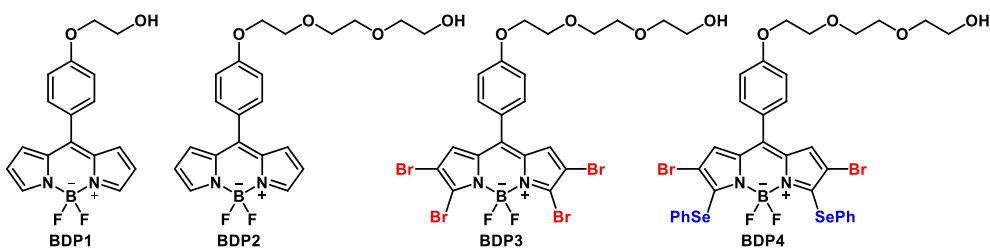


Fig. 1 Structures of BODIPYs used in this study.

3.1. Photophysical characterization of BODIPYs

All synthesized BODIPYs (**BDP1-BDP4**) were also characterized from a photophysical point of view through absorption, emission and excitation spectra (Fig. S1). Values were obtained for molar absorption coefficients (ϵ), Full width at half maximum ($Fwhm_{abs}$) and ($Fwhm_{em}$), Stokes shift ($\Delta\lambda$), maximum emission wavelength in solid state ($\lambda_{em\ solid}$) and fluorescence quantum yield (Φ_F). Analyzing the absorption spectra, it is possible to observe the presence of a more intense main band, located around 500 - 600 nm, corresponding to the $S_0 \rightarrow S_1$ transition and, at lower wavelengths (400 - 500 nm), there is a second band of lower intensity, corresponding to higher energy transitions ($S_0 \rightarrow S_n$, $n \geq 2$). [34],[35] This spectral profile is characteristic of BODIPY derivatives.[34],[35],[36],[37] In some cases (Fig. S1A, B, C), the presence of a shoulder in the main band can be observed, quite clearly in the case of **BDP3** (Fig. S1 C). This shoulder can be attributed to transitions in vibrational levels (0 - 1) and, depending on the molecule, can be pronounced.[34] For **BDP4** the spectral profile is wider due to the presence of the chalcogen atoms directly attached to the chromophoric nucleus, and this shoulder is not observed. The emission spectra for all the compounds appear as mirror images of the absorption spectra, corresponding to the $S_1 \rightarrow S_0$ transition. Excitation spectra for all compounds were obtained, and showed a similarity with the corresponding absorption spectra, indicating that the systems are free of fluorescent impurities. Large ϵ were obtained ($45827 - 115353\ L.mol^{-1}.cm^{-1}$, for the main band) for all compounds. Regarding fluorescence emission intensity, fluorescence quantum yield for all compounds were obtained (Table 1). Comparing the values obtained for **BDP1** and **BDP2**, it was noticed that the Φ_F decreases with the increase of the size of the upper portion derived from PEG, due to more rotational degrees of freedom favoring decays by non-radiative processes. However, when chalcogen is inserted into the BODIPY

structures (**BDP4**), a fluorescence quenching ($\Phi_F < 0.01$) is observed, due to the presence of the "SePh" group, as already reported in the literature.[38] It is known that the presence of these groups in the structure of the compound leads to fluorescence suppression through mechanisms such as Photoinduced electron Transfer (PeT).[38] It allows Seleno-BODIPYs, having their low fluorescence background, to be used as fluorescence *on/off* sensors for the detection of analytes which interact with SePh groups, such as anions, biothiols, cations, and nucleophiles, among others. [38],[39],[40],[41]

Table 1. Photophysical data of BODIPYs at 298 K

Compound	Absorption data			Emission data				
	λ_{abs} (nm)	ϵ (L.mol ⁻¹ .cm ⁻¹)	Fwhm _{abs} (nm)	λ_{em} (nm)	Fwhm _{em} (nm)	$\Delta\lambda$ (nm)	$\lambda_{\text{em solid}}$ (nm)	Φ
BDP1	387	11653	100.34766	512	29.80058	16	624	6.3 ^a
	496	45827	31.54985					
BDP2	383	20403	107.45315	511	29.65033	14	---	2.6 ^a
	497	64874	31.85047					
BDP3	435	24052	117.83221	562	28.06135	15	---	17.6 ^b
	547	115353	29.58737					
BDP4	458	18726	97.16779	628	46.47557	34	---	< 0.01
	594	68149	54.48659					

Absorption in solution (λ_{abs}), molar absorption coefficient (ϵ), full width at half maximum of absorption spectra (Fwhm_{abs}), emission maximum in solution (λ_{em}), full width at half maximum of emission spectra (Fwhm_{em}), Stokes shift ($\Delta\lambda$), emission maximum in the solid state ($\lambda_{\text{em solid}}$), fluorescence quantum yield (Φ_F) in solution. The solvent used was THF. **Conditions:** T = 298 K; [BODIPY] = 2 $\mu\text{mol/L}$. **BDP1** ($\lambda_{\text{ex}} = 465$ nm, $\lambda_{\text{em}} = 540$ nm, slit 2.5 nm), **BDP2** ($\lambda_{\text{ex}} = 480$ nm, $\lambda_{\text{em}} = 540$ nm, slit 2.5 nm), **BDP3** ($\lambda_{\text{ex}} = 520$ nm, $\lambda_{\text{em}} = 585$ nm, slit 2.5 nm), **BDP4** ($\lambda_{\text{ex}} = 570$ nm, slit 5.0 nm, $\lambda_{\text{em}} = 635$ nm, slit 10.0 nm). ^aFluorescein in NaOH (0.1 mol/L) ($\Phi = 92.5\%$) as standard, ^bRhodamine 6G in ethanol ($\Phi = 95.0\%$) as standard.[42]

Luminescent properties of the BODIPYs in solid state were studied using emission spectra. It is known that the luminescent properties of a solid depend on both intermolecular interactions and aggregation between molecules. It should be noted that only **BDP1** has solid-state fluorescence, and a red color can be observed under UV light (Fig. S1A). This red-shifted emission obtained through the crystal structure of **BDP1** ($\lambda = 624$ nm) compared to that in solution ($\lambda = 512$ nm) can be explained by aggregation-induced emission (AIE)[10] through the state of *J-aggregation*, reported in the literature for other BODIPY derivatives.[43],[44],[45] However, comparing the results in solid state (Fig. S1), it was verified that the presence of the longer upper chain influences the solid-state properties of the compound, promoting a quenching in emission of **BDP2** compared to **BDP1**. This could be explained by the increase in steric hindrance and in rotational degrees of freedom that the PEG chain brings to the molecule. In **BDP1**, as the

upper chain is short, this does not hinder the approximation between the molecules allowing *J-aggregation* to occur, resulting in emission in the solid state. By increasing the length of the upper chain, this approximation at a specific angle of the molecules is hindered, favoring the occurrence of aggregation-induced quenching (ACQ) in **BDP2**, leading to an increase in luminescence decay by non-radiative processes. ACQ is commonly seen in BODIPYs derivatives, resulting in low fluorescence emission in the solid state. In general, due to their the π -conjugated planar structure and small Stokes shift, BODIPYs derivatives can present self-absorption phenomena and strong $\pi - \pi$ stacking interactions, which contribute to the occurrence of solid-state ACQ, contrasting with their excellent photophysical properties in diluted solutions.[43],[12]

Functionalized compounds with voluminous and heavy atoms such as bromine (**BDP3**) and chalcogens (**BDP4**) show a significant spectral red-shift due to the heavy atom effect, with increasing $\Delta\lambda$ values.[46] Comparing **BDP1** and **BDP2**, the presence of the PEG-derived upper chain does not have significant effects on the spectroscopic properties of the compounds in solution (Fig. 2).

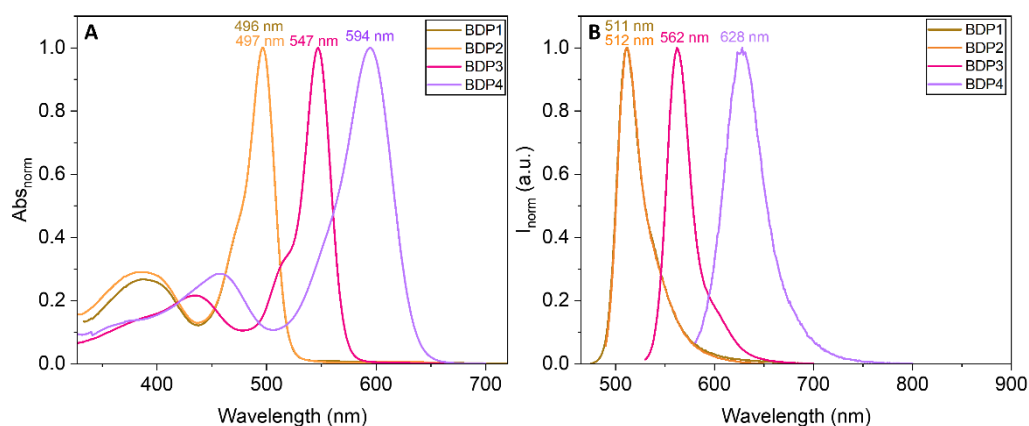


Fig. 2. **A)** Normalized absorption and **B)** emission spectra of compounds **BDP1**, **BDP2**, **BDP3**, and **BDP4** in THF. Conditions: T = 298 K; [BODIPY] = 2 μ mol/L. Conditions: **BDP1** (λ_{ex} = 465 nm, slit 2.5 nm), **BDP2** (λ_{ex} = 480 nm, slit 2.5 nm), **BDP3** (λ_{ex} = 520 nm, slit 2.5 nm), **BDP4** (λ_{ex} = 570 nm, slit 5.0 nm).

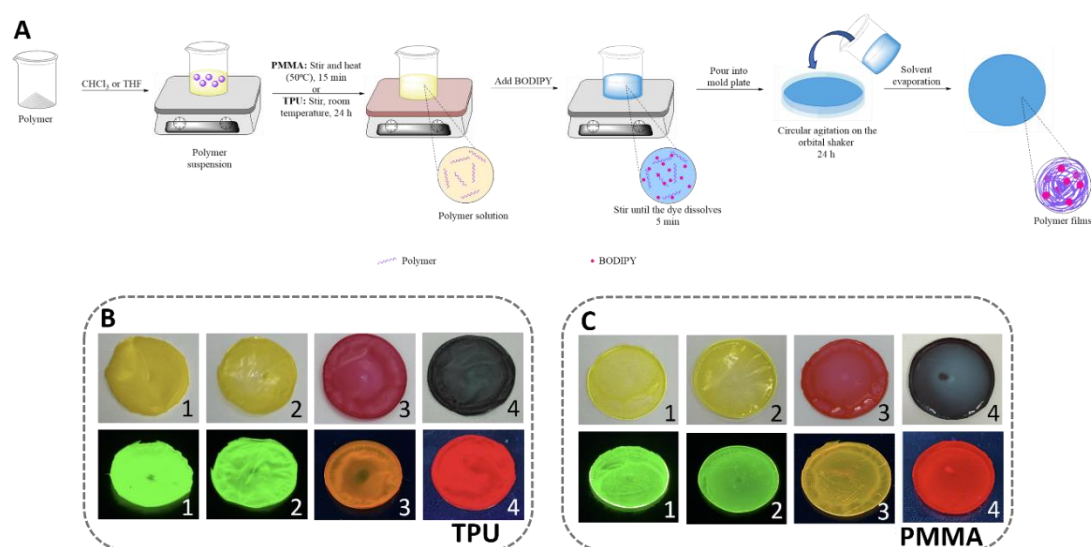
Organic compounds may exhibit high fluorescence emission in solution but decreased emission intensity or even total fluorescence quenching may be observed when in solid state. This may occur due to an intermolecular stacking by π - π interactions in the process of aggregation-induced quenching (ACQ).[43] **Fig. S1** shows that **BDP2-BDP4** were non-emissive in solid state. With future solid-state luminescent applications in mind, we incorporated all the compounds in polymeric matrices in a homogeneous way. The dye molecules remained dispersed in the polymeric matrix, avoiding the occurrence of ACQ

and enabling the emission of the compound incorporated in the polymeric film. The photophysical characterization of these new dye-doped polymer films with luminescent properties was performed.

3.2. Luminescent dye-doped polymer thin films

Thermoplastic polymers polyurethane (TPU) and poly(methyl methacrylate) (PMMA) were used as polymeric matrices to prepare the dye-doped polymer thin films. TPU was chosen due to its permeability, flexibility, elasticity, stretchability, moldability, and easy processability, in addition to other mechanical characteristics, which allows the obtaining of malleable dye-doped polymer.[47],[48] PMMA, a transparent, durable polymer with relatively low toxicity, is used in a wide range of applications, such as LCD screens, eyeglass lenses, implants, and solid-state dye laser.[49],[5],[50]

The film casting method[2],[51],[52] was used to incorporate the BODIPYs into the polymeric matrices to obtain the dye-doped polymer films. The procedure consisted of the initial dissolution of the polymer in a solvent (THF for TPU and CHCl_3 for PMMA), followed by the addition of BODIPY (previously solubilized in THF or CHCl_3) to the polymeric solution. After complete homogenization, the mixture is poured into a circular mold plate, under circular agitation, to allow a uniform solvent evaporation process. After drying, the polymer is demolded and is ready for analysis (Scheme 1). The final concentration obtained after dilution of the BODIPY solution in the polymeric solution obtained was $47 \mu\text{mol/L}$. This means that the % w/w of dye in each polymeric film varies between 0.17% w/w and 0.54% w/w; these can be considered low values, showing the excellent ability of the BODIPYs under study to be used as doping agents in these polymeric matrices.



Scheme 1. A) Synthesis of dye-doped polymer. B) Images of dye-doped polymer under visible light (above) and under UV light (below), using polymer matrix TPU and C) PMMA. Legend: 1) **BDP1**, 2) **BDP2**, 3) **BDP3**, 4) **BDP4**.

Images of the PMMA and TPU polymer films for each BODIPY under visible light and UV light are shown in Scheme 1B, C. As expected, the polymers doped with the compounds **BDP1**, **BDP2** and **BDP3** showed luminescence, as observed in solution, due to the dispersion of the molecules in the polymer matrix. To our surprise, **BDP4**, which did not show fluorescence in a diluted THF solution, when incorporated into the PMMA or TPU polymeric matrices showed a very intense luminescence with red color. This effect can be explained because when in solution, the presence of chalcogenated groups suppresses the fluorescence of the compound through the Photoinduced Electron Transfer (PeT) process, due to the electron-donating effect of the chalcogen to the BODIPY core.[53],[54],[55] The PeT process has been observed in other Seleno-BODIPY derivatives.[56],[39],[40] However, when in a polymeric film, the presence of selenium heteroatoms in the structure along with the substituent “SePh” aromatic rings probably induces the formation of aggregates resulting in aggregation-induced emission, producing an intense luminescence which blocks the PeT process. Examples involving an organic compound of selenium with aggregation-induced emission have been previously reported.[57] To the best of our knowledge, this is the first example of a fluorescent seleno-BODIPY incorporated in polymer films.

The normalized emission spectra were obtained for each BODIPY-doped polymer (Fig. S2); the emission maximums obtained are shown in Table 2. Analysis of the emission

spectra of each BODIPY in the two polymeric matrices shows in most cases a red-shift and a wider spectrum when in the TPU matrix compared to the PMMA matrix. This could be associated with the nature of each polymer matrix, their intrinsic properties, as well as the intermolecular interactions that the polymer may have with the dye.

The spectra obtained for **BDP1** and **BDP2** had very similar emission maxima (**BDP1@PMMA** = 516 nm and **BDP2@PMMA** = 516 nm; **BDP1@TPU** = 531 nm; and **BDP2@TPU** = 529 nm). Thus, as observed in the studies performed in solution, the size of the upper chain of BODIPY did not show significant effects on the luminescent properties of BODIPY-doped polymer films (Table 2).

Table 2. Emission maximum for all polymer doped with BODIPYs

Polymer	λ_{em} (nm)	Polymer	λ_{em} (nm)
BDP1@PMMA	516	BDP1@TPU	531
BDP2@PMMA	516	BDP2@TPU	529
BDP3@PMMA	570	BDP3@TPU	571
BDP4@PMMA	617	BDP4@TPU	648

A comparative analysis of the BODIPY-doped polymer films, varying the dye for each polymeric film (Fig. S3) in both PMMA and TPU, shows that the **BDP3** tetrabrominated BODIPY presents a bathochromic displacement compared to the spectra of BODIPYs without functionalization in the nucleus (**BDP1** and **BDP2**), as observed previously in solution (Fig. 2). It has been reported[46] that the nature of the substituent bound at positions 3 and 5 of the BODIPY nucleus can have a strong effect on the displacement of the absorption and emission maxima of the compound in solution. Thus, when introducing the electron donor groups "SePh" at positions 3 and 5 of the nucleus (**BDP4**), a red shift is observed.[58]

Overall, the new dye-doped polymer films showed good luminescent characteristics. Thus, we proceed to investigate their thermometric properties and thermostability, to ascertain their potential as possible temperature sensors.

3.3. Thermochromic behavior of the polymer materials

The thermal response of the new BODIPY-doped polymer films was explored through heating cycles, followed by cooling cycles, and monitored by luminescence emission spectra. The experiments were conducted for **BDP1-BDP4** incorporated into PMMA and TPU polymeric matrices. **BDP1** is here discussed as a representative example of the behavior of all the BODIPY-doped polymer films; the emission spectra for the

heating and cooling cycles for **BDP2-BDP4** are shown in Fig. S4-S6. **Fig. 3** shows the normalized emission spectra at variable temperatures for **BDP1@TPU (Fig 3 A, B)** and **BDP1@PMMA (Fig. 3 C, D)**. A decrease in emission intensity was observed with increasing temperature, as expected, since higher temperatures favor the occurrence of non-radiative processes, leading to the almost total extinction of the compound's luminescence. This can be better visualized in **Fig. 3 E (BDP1@TPU)** and **F (BDP1@PMMA)**, which show normalized intensity vs temperature at the maximum emission wavelength of each compound in the heating and cooling cycles. No significant changes were observed in the maximum emission wavelength of the compound after the cycle. Recovery of 74% for **BDP1@PMMA** and 57% for **BDP1@TPU** were obtained. **Fig. 4** shows that the heating cycles performed in TPU follow an exponential function adjustment, while for PMMA the adjustment is predominantly a linear function. In addition, it was noted that higher temperatures had to be used for PMMA films for luminescence extinction, compared to TPU films. This may be related to the differences in thermal conductivity (k) values for the two polymers. PMMA, has a higher k value (0.21 W/m.K)[59] than TPU (0.15 W/m.K)[60], which could contribute to an increase in dissipation heat, reducing luminescence decays by thermally activated non-radiative media, and causing higher energy to be necessary to observe fluorescence extinction. The TPU matrix is also more flexible, malleable, and porous than the PMMA one. After heating, TPU has a tendency to stretch elastically, allowing heat to penetrate more quickly into the TPU films than into the PMMA ones, which could cause a reorganization inside the film and thus result in a different behavior from that observed in PMMA. Furthermore, data for the heating stage of PMMA films can be adjusted to two straight lines, suggesting a 2-step process; the cooling stage occurs in just one step.

After each heating and cooling cycle, recovery values of BODIPY's emission intensity were obtained for each polymer (Table S1). Good recovery values, equal or greater than 50%, were observed. Despite the elasticity observed in TPU-based films, the linearity observed in the heating/cooling cycles for PMMA-based films and their high recovery values, ranging from 78-85% (see Table S1), make the BODIPY-doped PMMA films more suitable for potential application as molecular thermometers than their TPU counterparts.

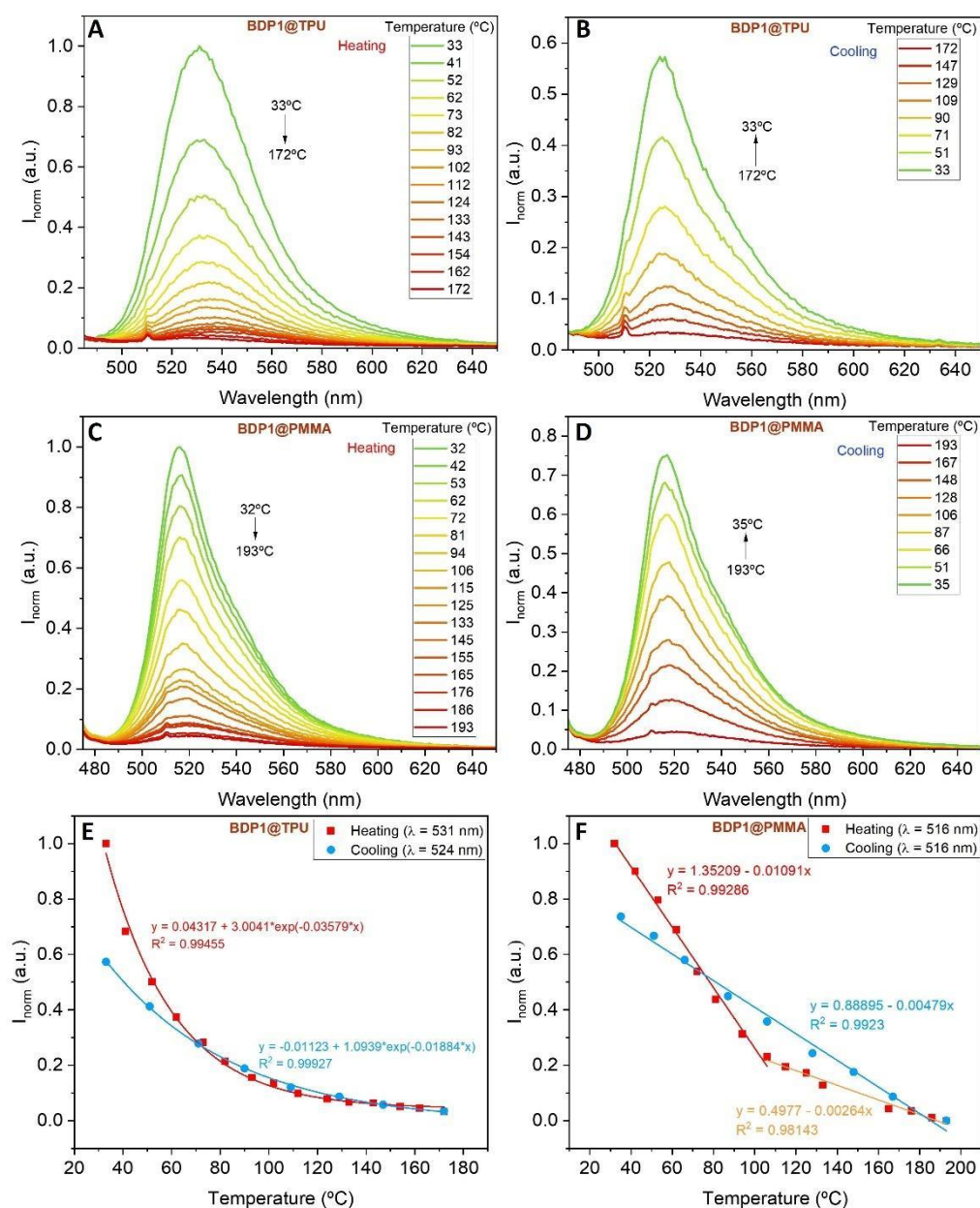


Fig. 3 Emission spectra of **BDP1@TPU** under **A**) heating (33°C to 172°C) and **B**) cooling (172°C to 33°C) obtained in different temperatures. Emission spectra of **BDP1@PMMA** under **C**) heating (32°C to 193°C) and **D**) cooling (193°C to 35°C) obtained in different temperatures. **E**) Correlation between normalized intensity of **BDP1@TPU** and temperature under heating ($\lambda = 531$ nm) and cooling ($\lambda = 524$ nm). **F**) Correlation between normalized intensity of **BDP1@PMMA** and temperature under heating and cooling ($\lambda = 516$ nm). $\lambda_{\text{ex}} = 465$ nm, slit 1.0 nm.

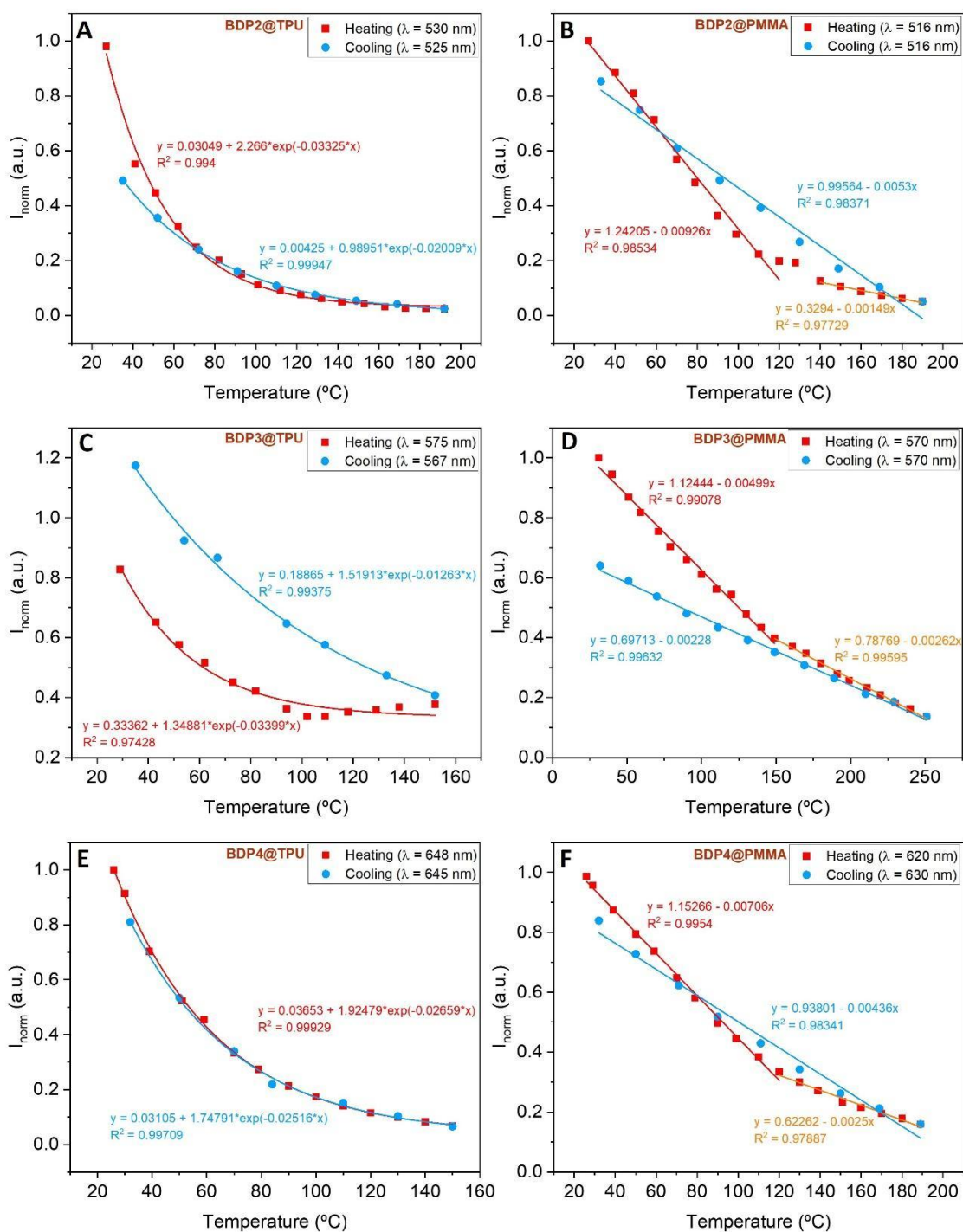


Fig. 4 **A)** Correlation between normalized intensity of **BDP2@TPU** and temperature under heating ($\lambda = 530$ nm) and cooling ($\lambda = 525$ nm). $\lambda_{ex} = 480$ nm, slit 1.0 nm. **B)** Correlation between normalized intensity of **BDP2@PMMA** and temperature under heating and cooling ($\lambda = 516$ nm). $\lambda_{ex} = 480$ nm, slit 1.0 nm. **C)** Correlation between normalized intensity of **BDP3@TPU** and temperature under heating ($\lambda = 575$ nm) and cooling ($\lambda = 567$ nm). $\lambda_{ex} = 520$ nm, slit 2.0 nm. **D)** Correlation between normalized intensity of **BDP3@PMMA** and temperature under heating and cooling ($\lambda = 570$ nm). $\lambda_{ex} = 520$ nm, slit 2.0 nm. **E)** Correlation between normalized intensity of **BDP4@TPU**

and temperature under heating ($\lambda = 648$ nm) and cooling ($\lambda = 645$ nm). $\lambda_{\text{ex}} = 570$ nm, slit 2.5 nm. **F)** Correlation between normalized intensity of **BDP4@PMMA** and temperature under heating ($\lambda = 620$ nm) and cooling ($\lambda = 630$ nm). $\lambda_{\text{ex}} = 570$ nm, slit 3.0 nm.

3.4. Polymer films behavior in NH_4OH solution

In order to explore potential applications of the new BODIPY-doped TPU polymeric films, we have tested their sensing capability towards NH_4OH . Samples of each TPU film were immersed in an NH_4OH solution (5.0 mol/L). Emission spectra of the solid polymers, obtained before and after reaction with NH_4OH , are shown in Fig. S7. For **BDP3@TPU** and **BDP4@TPU**, a reaction was observed, which resulted in the formation of yellow-fluorescent products (Fig 5); for BODIPYs **1** and **2**, no reaction was observed. **BDP4@TPU** was chosen to conduct kinetic studies with different concentrations of NH_4OH . The response of **BDP4@TPU** to 5 mol/L HCl was also studied; the tests conducted showed no significant visual response to the strongly acidic media (Fig. S8).

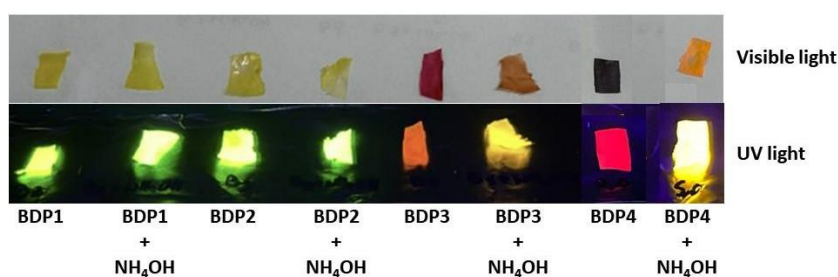


Fig 5. Images of BODIPY-doped TPU polymer, developed under visible light (above) and under UV light (below), before and after reaction with NH_4OH (5 mol/L, 1 hour).

3.5. Time-dependent response of BODIPY in NH_4OH solutions

Kinetic studies of the reaction between **BDP4@TPU** and NH_4OH were conducted using different concentrations of NH_4OH (0, 0.1, 0.5, 1.0, 2.5 and 5.0 mol/L). Pieces of the polymer film in the different solutions, and images of the polymer under visible light and UV light were taken after 10, 25, 30, 45, 60 and 100 min of reaction (Fig. 6).

Fig. 6 shows an abrupt color change of the polymer from blue to orange (under visible light) and from red to fluorescent yellow (under UV light), as the concentration of the analyte and the reaction time increased. For each time, emission spectra of the solid polymer were also recorded (Fig. S9).

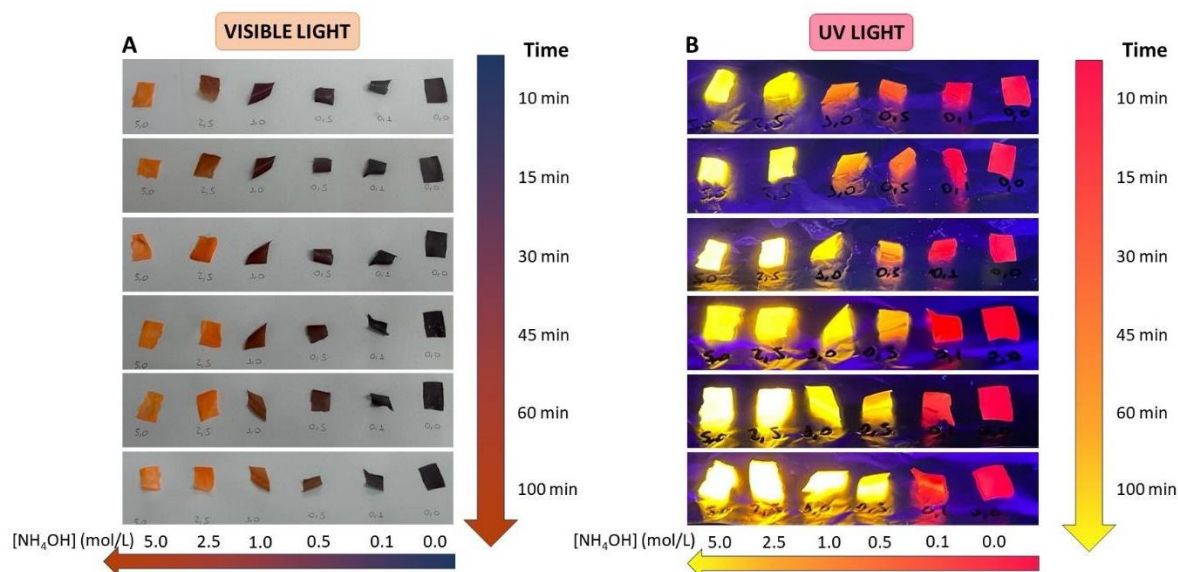


Fig. 6. Images of **BDP4@TPU** **A)** under visible light and **B)** under UV light after reaction with different concentrations of NH_4OH (0 – 5 mol/L) and reaction time (10 – 100 min).

Analysis of the polymeric films was carried out colorimetrically and fluorometrically. Software containing an RGB color detector (GIMP 2.10.24) was used to quantify signal intensity (**Fig. 7**). The red (R) parameter was chosen due to a greater variation between the extreme signals (0 to 5 mol/L of NH_4OH) under visible light (**7A**) and the green (G) parameter used to quantify under UV light (**7C**). A similar kinetic profile was also obtained in the solid-state emission spectrum of the polymer (**7E**). The variation in polymer coloration can also be clearly observed in the CIE graphs, by the conversion of R, G and blue (B) into Yxy values. Thus, as the **BDP4@TPU** submerged in NH_4OH reacts over time, a change in color from blue to red/orange was observed under visible light (**7B**), and from red to yellow under UV light (**7D**). Moreover, fluorometric analysis was conducted by obtaining the emission spectra of the solid polymers. The spectra show the conversion of the emission spectrum of **BDP4@TPU**, initially centered at 648 nm, to another peak at 575 nm after reaction with NH_4OH solution (Fig S9). Fig. S9 F shows that after 100 minutes at the highest concentration studied (5.0 mol/L) a degradation could take place, and the intensity of the emission is partially quenched. These results suggest that photographic analysis can be a very useful tool for the colorimetric studies of polymeric films, when compared with the results from fluorimetric analysis performed with a spectrofluorometer. There is good agreement between the results obtained by the two techniques (see Fig. 7A and 7E) and both are effective for the quantification of the studied analyte, NH_3 (aqueous NH_4OH). However, photographic images is particularly attractive as an easy, fast and low cost alternative to fluorimetric analysis, requiring only

a device capable of obtaining photographic images, such as a cellphone. This would allow analyses to be performed at the sample collection point.

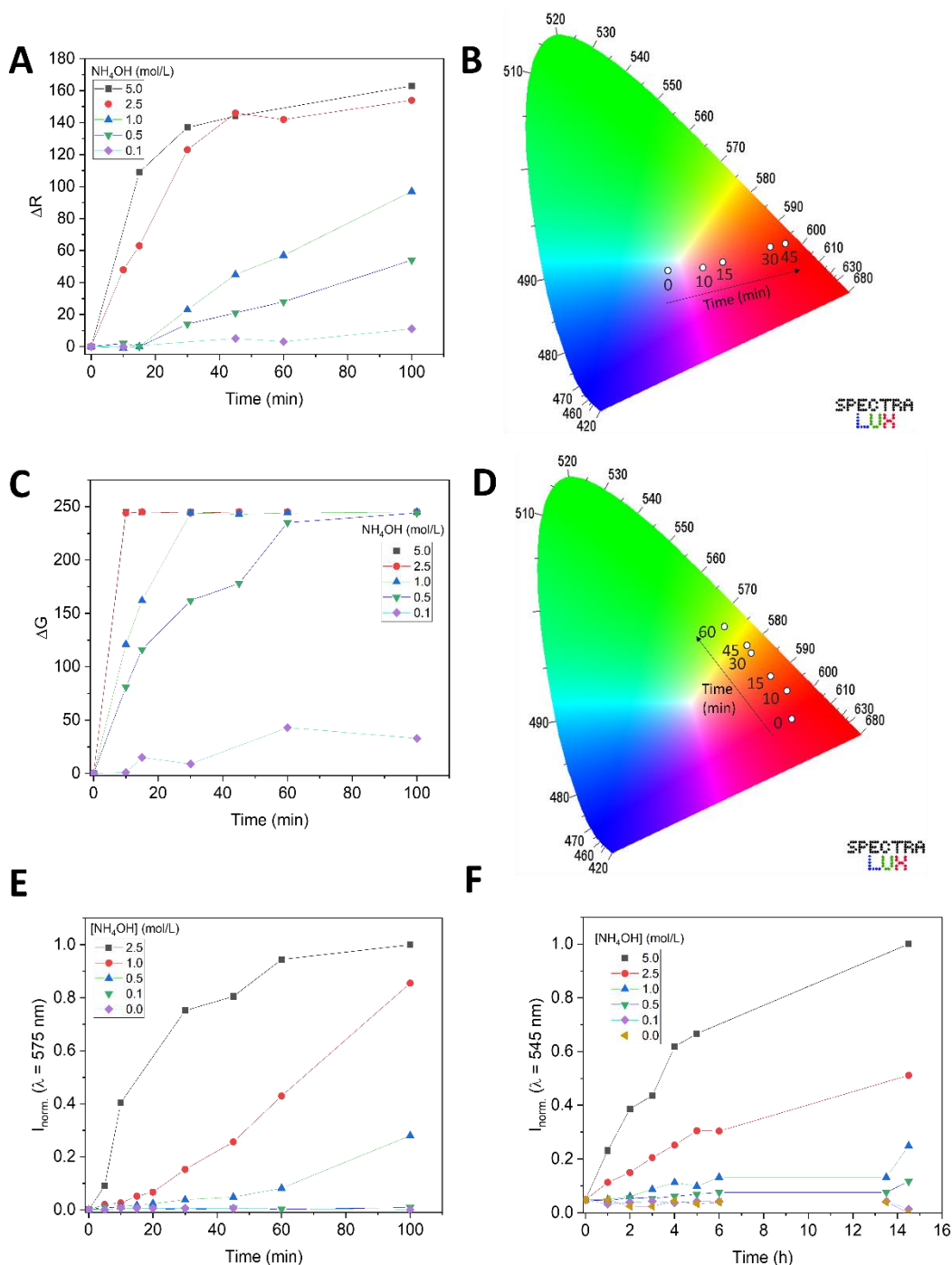


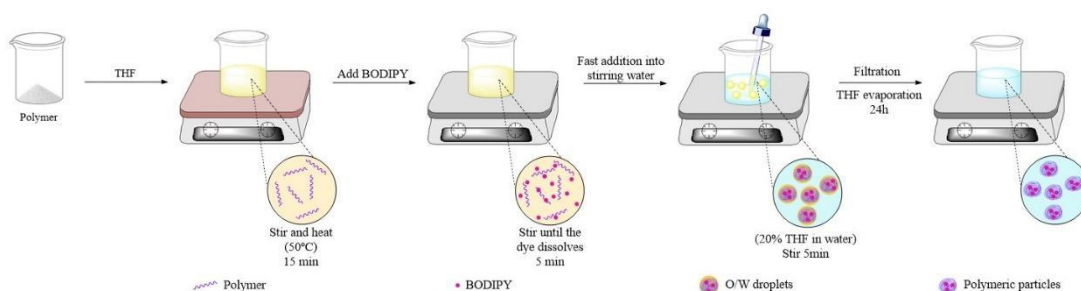
Fig. 7. **A)** Correlation between ΔR values (extracted from **Fig. 6A** under visible light) and time for **BDP4@TPU** after dipping in solutions containing different concentrations of NH_4OH (0 – 5 mol/L). **B)** CIE 1931 chromaticity diagram obtained through photography analysis from **Fig. 6A** (visible light) for **BDP4@TPU** under 1.0 mol/L of NH_4OH over time (0 – 45 min). **C)** Correlation between ΔG values (extracted from **Fig. 6B** (under UV light) and time for the **BDP4@TPU** after dipping in solutions containing different concentrations of NH_4OH (0 – 5 mol/L). **D)** CIE 1931 chromaticity diagram obtained

through photography analysis from **Fig. 6B** (under UV light) for **BDP4@TPU** under 0.5 mol/L of NH_4OH over time (0 – 60 min). **E**) Normalized intensity ($\lambda = 575 \text{ nm}$) of **BDP4@TPU** in function of time for the reaction with different concentrations of NH_4OH . **F**) Normalized intensity ($\lambda = 545 \text{ nm}$) of **BDP4@PMMA** in function of time for the reaction with different concentrations of NH_4OH .

A similar experiment was conducted with **BDP4-PMMA** (Fig. S10-S12). However, the reaction in PMMA is much slower than in TPU. Fluorimetric studies showed that it took more than 14 hours for the intensity to achieve a plateau, even at the highest concentration of NH_4OH studied (5 mol/L). This slower response of the PMMA polymer could be the result of the greater permeability of TPU when compared to PMMA, which would facilitate analyte entry.

3.6. Luminescent dye-doped polymer microparticles

In order to explore the potential of these materials in biomedical and biological applications, the BODIPYs were also incorporated into polymeric microparticles in water (see Scheme 2). First, the polymer was solubilized in THF. For PMMA, the solubilization procedure was carried out under heating and stirring for 15 minutes; TPU was solubilized in THF, under stirring, for 24 hours, without heating. The desired BODIPY was then added to the solution, and the mixture kept under stirring until complete solubilization of the BODIPY (5 minutes). The mixture was then quickly added to a flask containing water, under continuous stirring. After stirring, and filtration step, the organic solvent was left to evaporate for 24 hours. This procedure was applied to all the BODIPYs under study.



Scheme 2. Synthesis of polymeric microparticles of PMMA or TPU doped with BODIPYs.

All microparticles were characterized by DLS, zeta potential (Table S2), excitation and emission spectra (Fig. S13) and transmission electron microscopy (TEM). The Z-Average of particles doped with BODIPYs ranged from 182.6 nm to 247.6 nm (see Table S2). The polydispersity index (PDI) shows small particle size dispersion; the very negative zeta potential values obtained (-35.5 to -25.9 mV) show their good stability.

In addition, the insertion of BODIPYs into the particles resulted in an increased particle stability, as shown by the more negative zeta potential values compared to the controls. TEM images were obtained for BODIPYs encapsulated in TPU or PMMA polymers (Fig. S17-S20). Fig. 8 presents the results obtained for **BDP3** in PMMA particles (**BDP3(μ Ps)PMMA**). Results for **BDP4(μ Ps)PMMA** are shown in Fig. S18 and S19. Results from Energy Dispersive Spectroscopy (EDS) show the insertion of **BDP4** within the particles, with the presence of signals corresponding to the presence of bromine and selenium. TPU particles containing **BDP3** and **BDP4** were also analyzed showing that the particles were successfully obtained (Fig. S17 and S20). Knowing the low solubility of **BDP1** to **BDP4** in water, this strategy makes it possible to use them in completely aqueous media without precipitating the dye, facilitating further applications in biological media or environmental samples. In Fig. S14 it is possible to see the particles in aqueous solutions with the dye incorporated under visible and UV-light. Furthermore, we also decided to investigate the applicability of **BOD4(μ Ps)TPU** for the detection of ammonia in water.

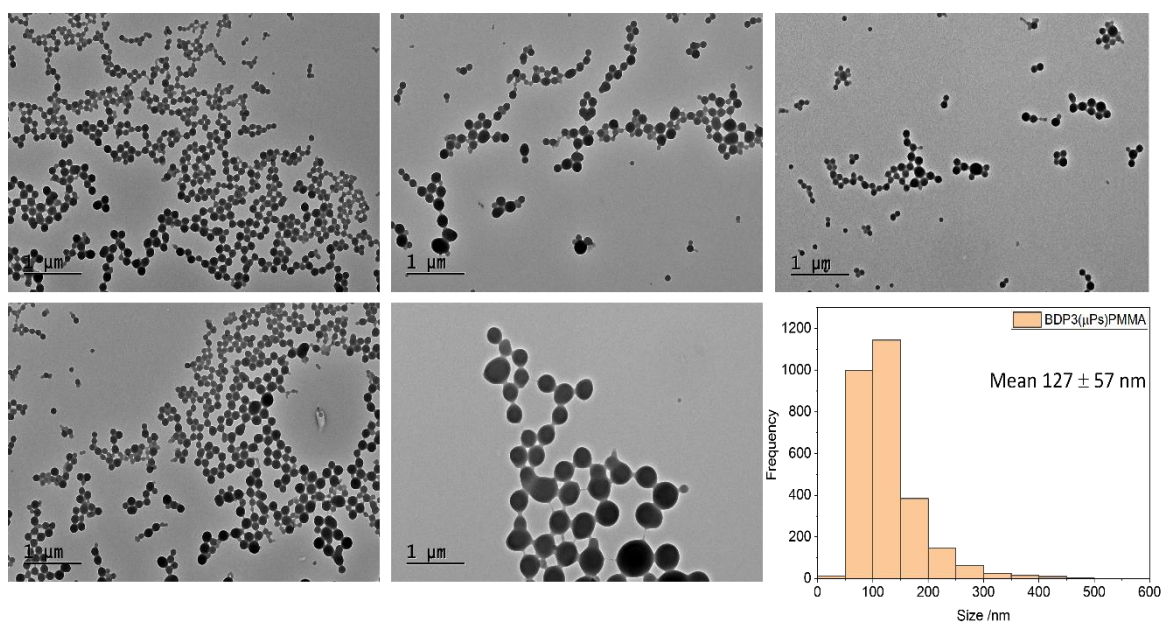


Fig. 8. Transmission electron microscopy (TEM) images of **BDP3(μ Ps)PMMA** particles and in the right a histogram of particle size distribution from TEM measurement of **BDP3(μ Ps)PMMA**.

3.7. Polymers particles behavior with NH_4OH solution

Several studies with **BDP4(μPs)TPU** in water were conducted to detect ammonia in solution using BODIPY-doped polymeric particles. Firstly, a kinetic study by absorption was conducted (**Fig. 9, Panel A**) and it was possible to verify that the reaction was completed after 3 hours, with the presence of an isosbestic point in the absorption spectra (Fig. S15). As the BODIPYs are now encapsulated inside the polymer particle, the reaction time is longer than in polymer films because in particles the reaction speed depends on the rate of permeability of the analyte to the interior of the particle, while in the polymer film the BODIPYs were dispersed on the surface of the material. A calibration curve using different concentrations of NH_4OH was obtained (**Fig. 9, Panel B, Fig. S16**), showing a linear correlation in the range of 0.00 to 0.75 mol/L of analyte ($y = 1.421x - 0.016$, $R^2 = 0.983$). The coloration of the aqueous solutions containing the polymeric particles changed from blue to light orange with the addition of increasing amounts of ammonia. In this way, it was possible to demonstrate the applicability of the sensor in aqueous media.

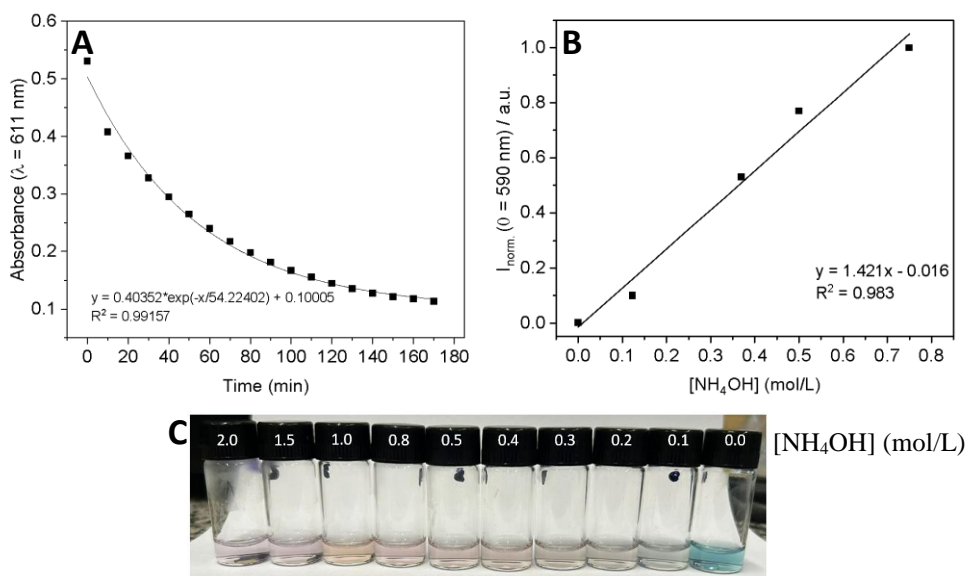
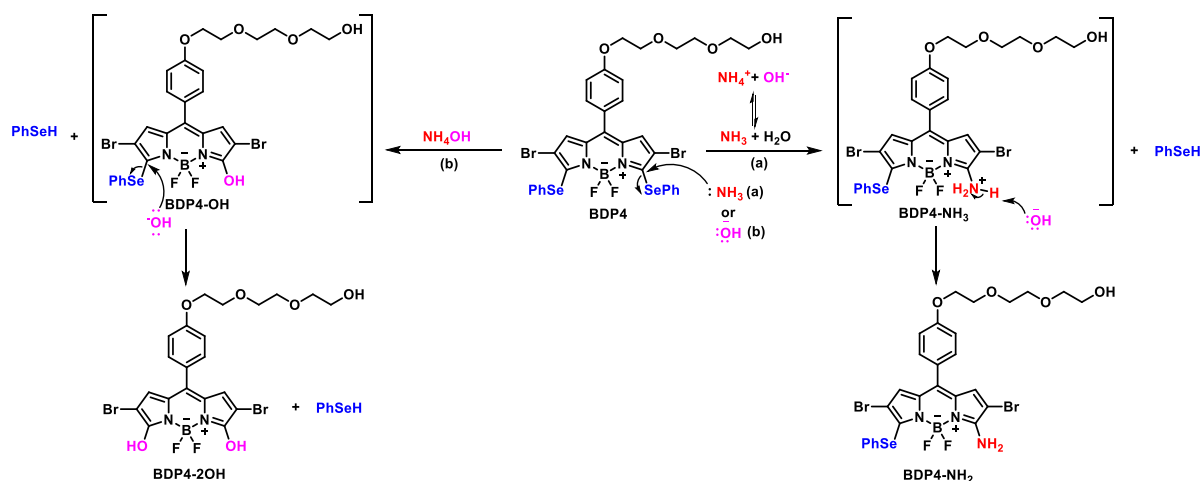


Fig. 9. **A)** Time-dependent absorption response of **BDP4(μPs)TPU** particles in water after addition of NH_4OH (0.59 mol/L). **B)** Calibration curve between fluorescence ($\lambda = 590 \text{ nm}$) of **BDP4(μPs)TPU** particles in water, after 3 hours of reaction. $\lambda_{\text{ex}} = 540$, slit 5.0 nm. **C)** Images of **BDP4(μPs)TPU** solutions in water containing different concentrations of NH_4OH (0 – 2 mol/L).

3.8. Reaction mechanism in NH_4OH solutions

HRMS analyses were conducted to investigate the reaction that occurred when **BDP4** is in the presence of NH_4OH solutions. The formation of **BDP4-NH₂** and **BDP4-2OH** products was observed. **BDP4-NH₂** originates from a nucleophilic attack by ammonia (present in the aqueous solution in equilibrium with ammonium hydroxide) to carbon 3 or 5 of the BODIPY nucleus. This attack leads to the formation of the **BDP4-NH₃** intermediate, with the leaving group "SePh" forming benzoselenol (PhSeH) in the aqueous medium; subsequent hydrogen abstraction results in the formation of compound **BDP4-NH₂**. Additionally, **BDP4** can undergo nucleophilic attack by OH^- . In this case, a double substitution of the "SePh" groups was observed, resulting in the formation of **BDP4-2OH** (Fig. S32 – S39). The isotopic profiles of the final products **BDP4-NH₂** and **BDP4-2OH** were obtained (Fig. S37, S39). It is noteworthy that Nucleophilic Aromatic Substitution of one "SePh" group at position 3 or 5 of the BODIPY nucleus, resulting in the insertion of an OH group, has already been observed in our group for a BODIPY derivative functionalized with four "SePh" groups.[31]

Furthermore, the absorption spectral profile obtained after the addition of NH_4OH into the **BDP4(μPs)TPU** dispersed in water was very similar to that obtained for **BDP4** in the presence of NH_4OH in THF (Fig. S21) in the absence of polymer. This shows that the phenomenon observed in the polymer matrix is in fact the reaction of **BDP4** with the ammonia (NH_3), as depicted in scheme 3.



Scheme 3: Reaction products obtained when **BDP4** is in the presence of ammonia aqueous solution (NH_4OH).

4. Conclusions

Eight new BODIPY-containing polymer films using TPU or PMMA as matrix were prepared, and their photophysical properties in the solid state were studied. The thermometric response of the BODIPY-containing polymers was explored by obtaining heating and cooling curves. Good luminescence recovery values (equal or greater than 50%) were observed after the heating/cooling cycles, indicating the reversibility of the process; these responses indicate the potential of these compounds to act as molecular thermometers. Although the TPU polymers are more malleable and elastic, the linearity obtained between emission intensity and temperature for PMMA derivatives, together with the high recovery values, make BODIPY-doped PMMA films better candidates for thermometric applications when compared to the TPU ones.

Studies of the reactivity of the films with aqueous ammonia solution (NH_4OH) were conducted. The brominated (**BDP3**) and chalcogenated (**BDP4**) BODIPYs responded to the analyte, resulting in yellow-fluorescent products with a blue spectral shift. Kinetic studies with **BDP4@TPU** and **BDP4@PMMA** were conducted, recording emission spectra and photographic images of the polymers after exposure to different concentrations of the analyte for different reaction times. The results obtained indicate that the reaction with ammonia in TPU matrix is much faster (100 minutes to complete) than with PMMA (more than 14 hours) due to differences in permeability of materials. The studies performed show that quantification by photographic analysis is a promising tool for monitoring BODIPY's reaction with ammonia in the polymer matrix. The photographic analysis method is fast, effective, portable, and cheap, and does not need sophisticated equipment to quantify the analyte. Finally, all BODIPYs were also encapsulated in polymeric particles, and **BDP4(μPs)TPU** was successfully applied in the detection of ammonia in water without the use of organic solvents.

5. Declaration of Competing Interest

The authors declare no conflict of interest.

6. Ethical Approval

No Ethical Approval was necessary.

7. Funding

Beatriz S. Cugnasca thanks FAPESP (2019/07634-1 and 2023/01092-8) for Ph.D. scholarship and CNPq (141855/2019-3). Alcindo A. Dos Santos thanks FAPESP (2018/24434-3) and CNPq. All authors thank FAPESP, CNPq, and CAPES for financial support and the Institute of Chemistry of University of São Paulo, Brazil for research structure and support. F.D. thanks to FCT/MCTES (Portugal) for his doctoral grant 2021.05161.BD. HMS acknowledges the Associate Laboratory for Green Chemistry-LAQV (LA/P/0008/2020) funded by FCT/MCTES for his research contract. This work received support and help from FCT/MCTES (LA/P/0008/2020 DOI 10.54499/LA/P/0008/2020, UIDP/50006/2020 DOI 10.54499/UIDP/50006/2020 and UIDB/50006/2020 DOI 10.54499/UIDB/50006/2020), through national funds. PROTEOMASS Scientific Society (Portugal) is acknowledged by the funding provided through the General Funding Grant 2023–2024, and by the funding provided to the Laboratory for Biological Mass Spectrometry – Isabel Moura (#PM001/2019 and #PM003/2016).

8. Acknowledgements

We thank Dr. Iolanda M. Cuccovia (IQ-USP) for her kind assistance in providing analytical instrumentations for DLS analysis, absorption and emission spectra of the dye doped particles. We thank also Prof. Dr. Shaker Chuck Farah and Michella Brescia Reátegui (IQ-USP) for helping with the hydrophilizing of the grids for TEM analysis. Thanks to Dr. Javier Fernández Lodeiro from the BIOSCOPE Research Group at the NOVA FCT for his expertise comments regarding the polymeric nanoparticles characterization.

9. Data Availability

All our data not included in the Supplementary Material are available upon request.

References

- [1] C. Fleischmann, M. Lievenbrück, H. Ritter, *Polymers and dyes: Developments and applications*, *Polymers* (Basel) 7 (2015) 717–746. <https://doi.org/10.3390/polym7040717>.
- [2] F. Duarte, G. Dobrikov, A. Kurutos, J.L. Capelo-Martinez, H.M. Santos, E. Oliveira, C. Lodeiro, Development of fluorochromic polymer doped materials as platforms for temperature sensing using three dansyl derivatives bearing a sulfur bridge, *J Photochem Photobiol A Chem* 445 (2023) 115033. <https://doi.org/10.1016/j.jphotochem.2023.115033>.
- [3] A. Reisch, A.S. Klymchenko, Fluorescent Polymer Nanoparticles Based on Dyes: Seeking Brighter Tools for Bioimaging, *Small* 12 (2016) 1968–1992. <https://doi.org/10.1002/smll.201503396>.
- [4] J. Li, J. Fan, R. Cao, Z. Zhang, J. Du, X. Peng, Encapsulated Dye/Polymer Nanoparticles Prepared via Miniemulsion Polymerization for Inkjet Printing, *ACS Omega* 3 (2018) 7380–7387. <https://doi.org/10.1021/acsomega.8b01151>.
- [5] A. Prakash, J.C. Janardhanan, V.K. Praveen, P. Radhakrishnan, A. Mujeeb, Multimode laser emission from BODIPY dye-doped polymer optical fiber, *J Lumin* 252 (2022) 119343. <https://doi.org/10.1016/j.jlumin.2022.119343>.
- [6] X. Zhang, K. Wang, M. Liu, X. Zhang, L. Tao, Y. Chen, Y. Wei, Polymeric AIE-based nanoprobes for biomedical applications: Recent advances and perspectives, *Nanoscale* 7 (2015) 11486–11508. <https://doi.org/10.1039/c5nr01444a>.
- [7] Q. Li, Z. Li, The Strong Light-Emission Materials in the Aggregated State: What Happens from a Single Molecule to the Collective Group, *Advanced Science* 4 (2017) 1600484. <https://doi.org/10.1002/advs.201600484>.
- [8] P. Bolle, T. Benali, C. Menet, M. Puget, E. Faulques, J. Marrot, P. Mialane, A. Dolbecq, H. Serier-Brault, O. Oms, J. Marrot, R. Dessapt, Tailoring the Solid-State Fluorescence of BODIPY by Supramolecular Assembly with Polyoxometalates, *Inorg Chem* 60 (2021) 12602–12609. <https://doi.org/10.1021/acs.inorgchem.1c01983>.
- [9] Y. Hong, J.W.Y. Lam, B.Z. Tang, Aggregation-induced emission, *Chem Soc Rev* 40 (2011) 5361–5388. <https://doi.org/10.1039/c1cs15113d>.
- [10] Y. Hong, J.W.Y. Lam, B.Z. Tang, Aggregation-induced emission: Phenomenon, mechanism and applications, *Chemical Communications* (2009) 4332–4353. <https://doi.org/10.1039/b904665h>.
- [11] H. Lu, Q. Wang, L. Gai, Z. Li, Y. Deng, X. Xiao, G. Lai, Z. Shen, Tuning the solid-state luminescence of bodipy derivatives with bulky arylsilyl groups: Synthesis and spectroscopic properties, *Chemistry - A European Journal* 18 (2012) 7852–7861. <https://doi.org/10.1002/chem.201200169>.
- [12] Y. Tang, B. Z. Tang, *Handbook of Aggregation-Induced Emission*, Wiley, 2022. <https://doi.org/10.1002/9781119643098>.

- [13] M. Plouzeau, S. Piogé, F. Peilleron, L. Fontaine, S. Pascual, Polymer/dye blends: Preparation and optical performance: A short review, 20 (2022) e52861. <https://doi.org/10.1002/app.52861>.
- [14] H. Maddali, A. M. Ryrshkin, D. M. O'Carroll, Dual-Mode Polymer-Based Temperature Sensor by Dedoping of Electrochemically Doped, Conjugated Polymer Thin Films, ACS Appl. Electron. Mater 3 (2021) 4718-4725. <https://doi.org/10.1021/acsaelm.1c00536>
- [15] Z. Ding, C. Wang, G. Feng, X. Zhang, Thermo-Responsive Fluorescent Polymers with Diverse LCSTs for Ratiometric Temperature Sensing through FRET, Polymers 10 (2018) 283. <https://doi.org/10.3390/polym10030283>
- [16] R. Diana, U. Caruso, F. S. Gentile, L. D., Costanzo, P. Musto, B. Panunzi, Structural feature of thermo-induced fluorochromism in a 1D zinc coordination polymer. A cross-analysis by PL and FTIR spectroscopy, and DFT formalism, Dyes and Pigments 202 (2022) 110247. <https://doi.org/10.1016/j.dyepig.2022.110247>
- [17] M. A. Ward, T. K. Georgiou, Thermoresponsive Polymers for Biomedical Applications, Polymers 3 (2011) 1215-1242. <https://doi.org/10.3390/polym3031215>
- [18] G. Pedro, F. Duarte, G. M. Dobrikov, A. Kurutos, H. M. Santos, J. L. Capelo-Martínez, E. Oliveira, C. Lodeiro, Dyes and Pigments 224 (2024) 112042. <https://doi.org/10.1016/j.dyepig.2024.112042>
- [19] G. Pedro, F. Duarte, D. A. Cheptsov, N. Y. Volodin, I. V. Ivanov, H. M. Santos, J. L. Capelo-Martínez, C. Cuerva, E. Oliveira, V. F. Traven, C. Lodeiro, Sensors 23 (2023) 1689. <https://doi.org/10.3390/s23031689>
- [20] N.R. Visaveliya, J.M. Köhler, Softness Meets with Brightness: Dye-Doped Multifunctional Fluorescent Polymer Particles via Microfluidics for Labeling, Adv Opt Mater 9 (2021) 2002219. <https://doi.org/10.1002/adom.202002219>.
- [21] K. Trofymchuk, J. Valanciunaite, B. Andreiuk, A. Reisch, M. Collot, A.S. Klymchenko, BODIPY-loaded polymer nanoparticles: Chemical structure of cargo defines leakage from nanocarrier in living cells, J Mater Chem B 7 (2019) 5199–5210. <https://doi.org/10.1039/c8tb02781a>.
- [22] The Royal Society, Ammonia: Zero-Carbon Fertiliser, Fuel and Energy Store. Policy Briefing. The Royal Society, London (2020).
- [23] P.R. Lakshmi, B. Mohan, P. Kang, P. Nanjan, S. Shanmugaraju, Recent advances in fluorescence chemosensors for ammonia sensing in the solution and vapor phases, Chemical Communications 59 (2023) 1728–1743. <https://doi.org/10.1039/d2cc06529k>.
- [24] R. P. Padappayil, J. Borger, Ammonia Toxicity, [Updated 2023 Mar11]. In: StatPearls [Internet]. Treasure Island (FL): StatPearls Publishing; 2024 Jan-. Available from: <https://www.ncbi.nlm.nih.gov/books/NBK546677/>
- [25] G.B. Guseva, E. V. Antina, M.B. Berezin, A.S. Smirnova, R.S. Pavelyev, I.R. Gilfanov, O.G. Shevchenko, S. V. Pestova, E.S. Izmet'sev, S.A. Rubtsova, O. V. Ostolopovskaya, S. V. Efimov, V. V. Klochkov, I.Z. Rakhmatullin, A.F. Timerova, I.A. Khodov, O.A. Lodochnikova, D.R. Islamov, P. V. Dorovatovskii, L.E. Nikitina, S. V. Boichuk, Design,

Spectral Characteristics, Photostability, and Possibilities for Practical Application of BODIPY FL-Labeled Thiosterpenoid, *Bioengineering* 9 (2022) 210. <https://doi.org/10.3390/bioengineering9050210>.

- [26] X. Ji, Y. Cai, X. Dong, W. Wu, W. Zhao, Selection of an aggregation-caused quenching-based fluorescent tracer for imaging studies in nano drug delivery systems, *Nanoscale* 15 (2023) 9290–9296. <https://doi.org/10.1039/d3nr01018j>.
- [27] R. Jiménez, F. Duarte, S. Nuti, J.A. Campo, C. Lodeiro, M. Cano, C. Cuerva, Thermochromic and acidochromic properties of polymer films doped with pyridyl- β -diketonate boron(III) complexes, *Dyes and Pigments* 177 (2020) 108272. <https://doi.org/10.1016/j.dyepig.2020.108272>.
- [28] B. González-Tobío, F. Duarte, A. Arribas-Delgado, C. Fernández-Lodeiro, J. Fernández-Lodeiro, M. Cano, C. Lodeiro, C. Cuerva, Tuning and reviving the luminescence of a new class of pyridyl β -diketonate Eu(III) metallomesogens: From molecules to entrapment in polymer particles, *Dyes and Pigments* 204 (2022) 110440. <https://doi.org/10.1016/j.dyepig.2022.110440>.
- [29] F. Duarte, C. Cuerva, C. Fernández-Lodeiro, J. Fernández-Lodeiro, R. Jiménez, M. Cano, C. Lodeiro, Polymer micro and nanoparticles containing B(III) compounds as emissive soft materials for cargo encapsulation and temperature-dependent applications, *Nanomaterials* 11 (2021) 3437. <https://doi.org/10.3390/nano11123437>.
- [30] B.S. Cugnasca, F. Wodtke, A.A. Dos Santos, Seleno-Functionalization of BODIPY Fluorophores Assisted by Oxidative Nucleophilic Hydrogen Substitution, *Curr Chem Biol* 15 (2021) 215–221. <https://doi.org/10.2174/2212796815666210504084205>.
- [31] B.S. Cugnasca, F. Duarte, J.L. Petrarca de Albuquerque, J. Luis Capelo-Martínez, C. Lodeiro, A.A. Dos Santos, Precision Detection of Cyanide, Fluoride, and Hydroxide ions Using a new Tetraseleno-BODIPY Fluorescent Sensor, *Journal of Photochemistry and Photobiology A: Chemistry* 457 (2024) 115881. <https://doi.org/10.1016/j.jphotochem.2024.115881>
- [32] B.S. Cugnasca, H.M. Santos, F. Duarte, J. Luis Capelo-Martínez, A.A. Dos Santos, C. Lodeiro, Fluorescent Discrimination of Cysteine, Homocysteine, and Glutathione in Urine Samples Using a novel Seleno-BODIPY Probe, 2024, *in press*.
- [33] S. Fery-forgues, D. Lavabre, Are Fluorescence Quantum Yields So Tricky to Measure? A Demonstration Using Familiar Stationery Products, *Journal of Chemical Education* 76 (1999) 1260.
- [34] K. Zlatić, H.B. El Ayouchia, H. Anane, B. Mihaljević, N. Basarić, T. Rohand, Spectroscopic and photophysical properties of mono- and dithiosubstituted BODIPY dyes, *J Photochem Photobiol A Chem* 388 (2020) 112206. <https://doi.org/10.1016/j.jphotochem.2019.112206>.
- [35] W. Qin, M. Baruah, M. Van Der Auweraer, F.C. De Schryver, N. Boens, Photophysical properties of borondipyrromethene analogues in solution, *Journal of Physical Chemistry A* 109 (2005) 7371–7384. <https://doi.org/10.1021/jp052626n>.

- [36] P. Rybczynski, A. Smolarkiewicz-Wyczachowski, J. Piskorz, S. Bocian, M. Ziegler-Borowska, D. Kędziera, A. Kaczmarek-Kędziera, Photochemical properties and stability of bodipy dyes, *Int J Mol Sci* 22 (2021) 6735. <https://doi.org/10.3390/ijms22136735>.
- [37] W. Qin, T. Rohand, M. Baruah, A. Stefan, M. Van Der Auweraer, W. Dehaen, N. Boens, Solvent-dependent photophysical properties of borondipyrromethene dyes in solution, *Chem Phys Lett* 420 (2006) 562–568. <https://doi.org/10.1016/j.cplett.2005.12.098>.
- [38] R. Mangain, F. V. Singh, Selenium-Based Fluorescence Probes for the Detection of Bioactive Molecules, *ACS Organic and Inorganic Au* 2 (2022) 262–288. <https://doi.org/10.1021/acsorginorgau.1c00047>.
- [39] S. V. Mulay, T. Yudhistira, M. Choi, Y. Kim, J. Kim, Y.J. Jang, S. Jon, D.G. Churchill, Substituent Effects in BODIPY in Live Cell Imaging, *Chem Asian J* 11 (2016) 3598–3605. <https://doi.org/10.1002/asia.201601400>.
- [40] T. Yang, J. Fan, Y. He, Y. Han, A selenium-based fluorescent probe for the sensitive detection of hypochlorous acid and its application in cell and zebrafish imaging, *J Photochem Photobiol A Chem* 447 (2024) 115253. <https://doi.org/10.1016/j.jphotochem.2023.115253>.
- [41] L.Y. Niu, Q.Q. Yang, H.R. Zheng, Y.Z. Chen, L.Z. Wu, C.H. Tung, Q.Z. Yang, BODIPY-based fluorescent probe for the simultaneous detection of glutathione and cysteine/homocysteine at different excitation wavelengths, *RSC Adv* 5 (2015) 3959–3964. <https://doi.org/10.1039/c4ra13526a>.
- [42] D. Magde, R. Wong, P.G. Seybold, Fluorescence Quantum Yields and Their Relation to Lifetimes of Rhodamine 6G and Fluorescein in Nine Solvents: Improved Absolute Standards for Quantum Yields, *Photochem Photobiol* 75 (2007) 327–334. [https://doi.org/10.1562/0031-8655\(2002\)0750327fqyatr2.0.co2](https://doi.org/10.1562/0031-8655(2002)0750327fqyatr2.0.co2).
- [43] Z. Liu, Z. Jiang, M. Yan, X. Wang, Recent Progress of BODIPY Dyes With Aggregation-Induced Emission, *Front Chem* 7 (2019). <https://doi.org/10.3389/fchem.2019.00712>.
- [44] C. Duan, Y. Zhou, G.G. Shan, Y. Chen, W. Zhao, D. Yuan, L. Zeng, X. Huang, G. Niu, Bright solid-state red-emissive BODIPYs: facile synthesis and their high-contrast mechanochromic properties, *J Mater Chem C Mater* 7 (2019) 3471–3478. <https://doi.org/10.1039/c8tc06421k>.
- [45] K. Li, X. Duan, Z. Jiang, D. Ding, Y. Chen, G.Q. Zhang, Z. Liu, J-aggregates of meso-[2.2]paracyclophanyl-BODIPY dye for NIR-II imaging, *Nat Commun* 12 (2021) 2376. <https://doi.org/10.1038/s41467-021-22686-z>.
- [46] E. Fron, E. Coutiño-Gonzalez, L. Pandey, M. Sliwa, M. Van Der Auweraer, F.C. De Schryver, J. Thomas, Z. Dong, V. Leen, M. Smet, W. Dehaen, T. Vosch, Synthesis and photophysical characterization of chalcogen substituted BODIPY dyes, *New Journal of Chemistry* 33 (2009) 1490–1496. <https://doi.org/10.1039/b900786e>.
- [47] Anju, R.S. Yadav, P. Pötschke, J. Pionteck, B. Krause, I. Kuřitka, J. Vilcakova, D. Skoda, P. Urbánek, M. Machovsky, M. Masař, M. Urbánek, M. Jurca, L. Kalina, J. Havlica, High-Performance, Lightweight, and Flexible Thermoplastic Polyurethane Nanocomposites with Zn²⁺-Substituted CoFe₂O₄Nanoparticles and Reduced Graphene

Oxide as Shielding Materials against Electromagnetic Pollution, *ACS Omega* 6 (2021) 28098–28118. <https://doi.org/10.1021/acsomega.1c04192>.

- [48] E. Seo, J. Choi, B. Lee, Y.A. Son, K.J. Lee, Dye Clicked Thermoplastic Polyurethane as a Generic Platform toward Chromic-Polymer Applications, *Sci Rep* 9 (2019) 18648. <https://doi.org/10.1038/s41598-019-54832-5>.
- [49] S.M. El-Bashir, M.S. AlSalhi, F. Al-Faifi, W.K. Alenazi, Spectral properties of PMMA films doped by perylene dyestuffs for photoselective greenhouse cladding applications, *Polymers (Basel)* 11 (2019) 494. <https://doi.org/10.3390/polym11030494>.
- [50] M. Jachak, R. Bhise, A. Chaturvedi, V. Kamble, G. Shankarling, Pyrroloquinoline Based Styryl Dyes Doped PMMA, PS, and PS/TiO₂ Polymer for Fluorescent Applications, *J Inorg Organomet Polym Mater* 32 (2022) 2441–2454. <https://doi.org/10.1007/s10904-022-02285-1>.
- [51] F. Duarte, K. Morice, T. Ghanem, D. Puchán Sánchez, P. Blanchard, C. S. B. Gomes, S. Herrero, C. Cabanetos, C. Cuerva, J. Luis Capelo-Martinez, C. Lodeiro, Harnessing liquid crystal attributes of near-unit photoluminescent benzothioxanthene photosensitizers: Photophysical profiling in solution, solid state, and polymer matrix embedding, *J Mol Liq* 409 (2024) 125424. <https://doi.org/10.1016/j.molliq.2024.125424>.
- [52] F. Duarte, G. Dobrikov, A. Kurutos, H.M. Santos, J. Fernández-Lodeiro, J.L. Capelo-Martinez, E. Oliveira, C. Lodeiro, Enhancing water sensing via aggregation-induced emission (AIE) and solvatofluorochromic studies using two new dansyl derivatives containing a disulfide bound: Pollutant metal ions detection and preparation of water-soluble fluorescent polymeric particles, *Dyes and Pigments* 218 (2023) 111428. <https://doi.org/10.1016/j.dyepig.2023.111428>.
- [53] S. V. Mulay, M. Choi, Y.J. Jang, Y. Kim, S. Jon, D.G. Churchill, Enhanced Fluorescence Turn-on Imaging of Hypochlorous Acid in Living Immune and Cancer Cells, *Chemistry - A European Journal* 22 (2016) 9642–9648. <https://doi.org/10.1002/chem.201601270>.
- [54] A. Loudet, K. Burgess, BODIPY dyes and their derivatives: Syntheses and spectroscopic properties, *Chem Rev* 107 (2007) 4891–4932. <https://doi.org/10.1021/cr078381n>.
- [55] A. Abdillah, P.M. Sonawane, D. Kim, D. Mametov, S. Shimodaira, Y. Park, D.G. Churchill, Discussions of fluorescence in selenium chemistry: Recently reported probes, particles, and a clearer biological knowledge†, *Molecules* 26 (2021) 692. <https://doi.org/10.3390/molecules26030692>.
- [56] R. Mamgain, F. V. Singh, Selenium-Based Fluorescence Probes for the Detection of Bioactive Molecules, *ACS Organic and Inorganic Au* 2 (2022) 262–288. <https://doi.org/10.1021/acsoinorgau.1c00047>.
- [57] T. Li, S. Pan, H. Zhuang, S. Gao, H. Xu, Selenium-Containing Carrier-Free Assemblies with Aggregation-Induced Emission Property Combine Cancer Radiotherapy with Chemotherapy, *ACS Appl Bio Mater* 3 (2020) 1283–1292. <https://doi.org/10.1021/acsaabm.9b01172>.

- [58] A. Bourouina, M. Rekhis, M. Trari, DFT/TD-DFT study of ruthenium bipyridyl-based dyes with a chalcogen donor (X = S, Se, Te), for application as dye-sensitized solar cells, *Polyhedron* 127 (2017) 217–224. <https://doi.org/10.1016/j.poly.2017.01.061>.
- [59] J.E. Mark, *Physical properties of polymer handbook*, Springer, 2006.
- [60] B. Pinedo, M. Hadfield, I. Tzanakis, M. Conte, M. Anand, Thermal analysis and tribological investigation on TPU and NBR elastomers applied to sealing applications, *Tribol Int* 127 (2018) 24–36. <https://doi.org/10.1016/j.triboint.2018.05.032>.